Status of the 2002 G^0 Commissioning Run

P. M. King
University Of Maryland, College Park

Participating institutions: California Institute of Technology, Carnegie-Mellon University, College of William and Mary, Hampton University, L'Institut de Physique Nucléaire d'Orsay, L'Institut des Sciences Nucléaires de Grenoble, Louisiana Tech. University, New Mexico State University, Thomas Jefferson National Laboratory, TRIUMF, University of Connecticut, University of Illinois at Urbana-Champaign, University of Kentucky, University of Manitoba, University of Maryland, University of Massachusetts, University of Northern British Columbia, Virginia Tech, and Yerevan Physics Institute

The G^0 Experiment is supported by the U.S. National Science Foundation (NSF) under grant PHY94-10768, the U.S. Department of Energy (DOE), the Natural Sciences and Engineering Research Council (NSERC) of Canada, and the Centre National de la Recherche Scientifique (CNRS) of France through the Institut National de Physique Nucléaire et de Physique des Particules (IN2P3).

Why Do Parity Violating e-N Scattering?

- Several areas of research of the nucleon (DIS, pDIS, $\pi - N$) have indicated that the sea quarks could play a significant role in the nucleon properties;
- Strange quarks are the lightest quark flavor which do not contribute to the nucleon valence distributions;
- The strange sea contributions to the nucleon properties are therefore of interest.

- Parity violating electron-nucleon scattering can be used to determine the neutral weak form factors of the nucleon, as the parity violating terms are due to weak interaction;
- In combination with the electromagnetic form factors, the neutral weak form factors allow decomposition of the nucleon form factors into flavor specific functions for the u, d, and s quarks.

- Several completed or proposed experiments provide data on the strange nucleon form factors through this technique;
- The G^0 experiment is the most ambitious, planning to measure the weak form factors and perform an independent extraction of the nucleon's strange form factors over a Q^2 range of 0.1 - 1.0 $(\mathrm{GeV}/c)^2$.

Formalism of PV e-N scattering

$A =$ 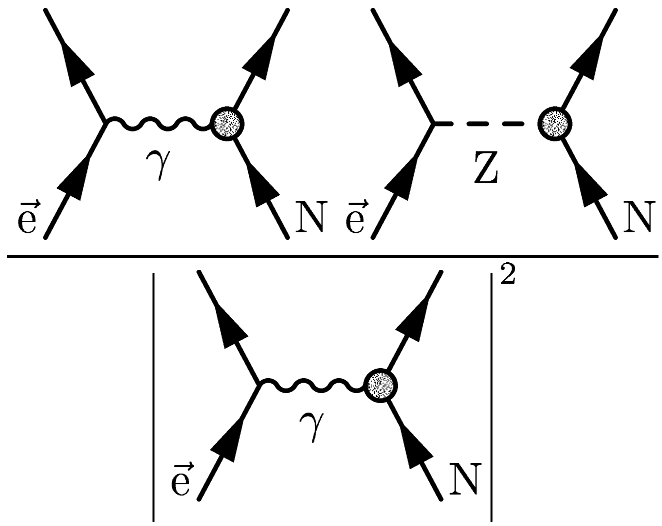

$= \frac{d\sigma_R - d\sigma_L}{d\sigma_R + d\sigma_L}$

$$A = -\frac{G_F Q^2}{4\sqrt{2}\pi\alpha}\frac{\varepsilon G_E^\gamma G_E^Z + \tau G_M^\gamma G_M^Z - (1 - 4\sin^2\theta_W)\varepsilon' G_M^\gamma G_A^e}{\varepsilon (G_E^\gamma)^2 + \tau (G_M^\gamma)^2}$$

$$\frac{G_F Q^2}{4\sqrt{2}\pi\alpha} \approx 5 \times 10^{-6}$$

Known kinematic factors: τ, ε, ε'.

Known electromagnetic form factors: $G_E^{\gamma,p}$, $G_M^{\gamma,p}$, $G_E^{\gamma,n}$, $G_M^{\gamma,n}$.

Use Rosenbluth separation techniques to extract the neutral weak form factors, G_E^Z, G_M^Z, G_A^e:

- Small scattering angles ($\varepsilon \to 1$)—A is sensitive to G_E^Z and G_M^Z.
- Large scattering angles—A is sensitive to G_M^Z and G_A^e.
- Either a third angle or a different nucleus can be used to separate G_M^Z and G_A^e.

Extraction of the Flavor Form Factors

$$A = -\frac{G_F Q^2}{4\sqrt{2}\pi\alpha} \frac{\varepsilon G_E^\gamma G_E^Z + \tau G_M^\gamma G_M^Z - (1 - 4\sin^2\theta_W)\varepsilon' G_M^\gamma G_A^e}{\varepsilon (G_E^\gamma)^2 + \tau (G_M^\gamma)^2}$$

Assuming charge symmetry:

$$G_{E,M}^{\gamma,p} = \frac{2}{3} G_{E,M}^u - \frac{1}{3} G_{E,M}^d - \frac{1}{3} G_{E,M}^s$$

$$G_{E,M}^{\gamma,n} = \frac{2}{3} G_{E,M}^d - \frac{1}{3} G_{E,M}^u - \frac{1}{3} G_{E,M}^s$$

$$G_{E,M}^{Z,p} = (1 - \frac{8}{3}\sin^2\theta_W) G_{E,M}^u + (-1 + \frac{4}{3}\sin^2\theta_W) G_{E,M}^d + (-1 + \frac{4}{3}\sin^2\theta_W) G_{E,M}^s$$

To lowest order:

$$G_{E,M}^{Z,p} = (1 - 4\sin^2\theta_W) G_{E,M}^{\gamma,p} - G_{E,M}^{\gamma,n} - G_{E,M}^s$$

$$A = \eta + \xi G_E^s + \chi G_M^s + \phi G_A^e$$

To do a complete separation (at a constant Q^2), three asymmetries are needed:

$$\begin{pmatrix} A_F \\ A_B \\ A_d \end{pmatrix} = \begin{pmatrix} \xi_F & \chi_F & \phi_F \\ \xi_B & \chi_B & \phi_B \\ \xi_d & \chi_d & \phi_d \end{pmatrix} \begin{pmatrix} G_E^s \\ G_M^s \\ G_A^e \end{pmatrix} + \begin{pmatrix} \eta_F \\ \eta_B \\ \eta_d \end{pmatrix}$$

G^0 Measurements and Kinematic Coverage

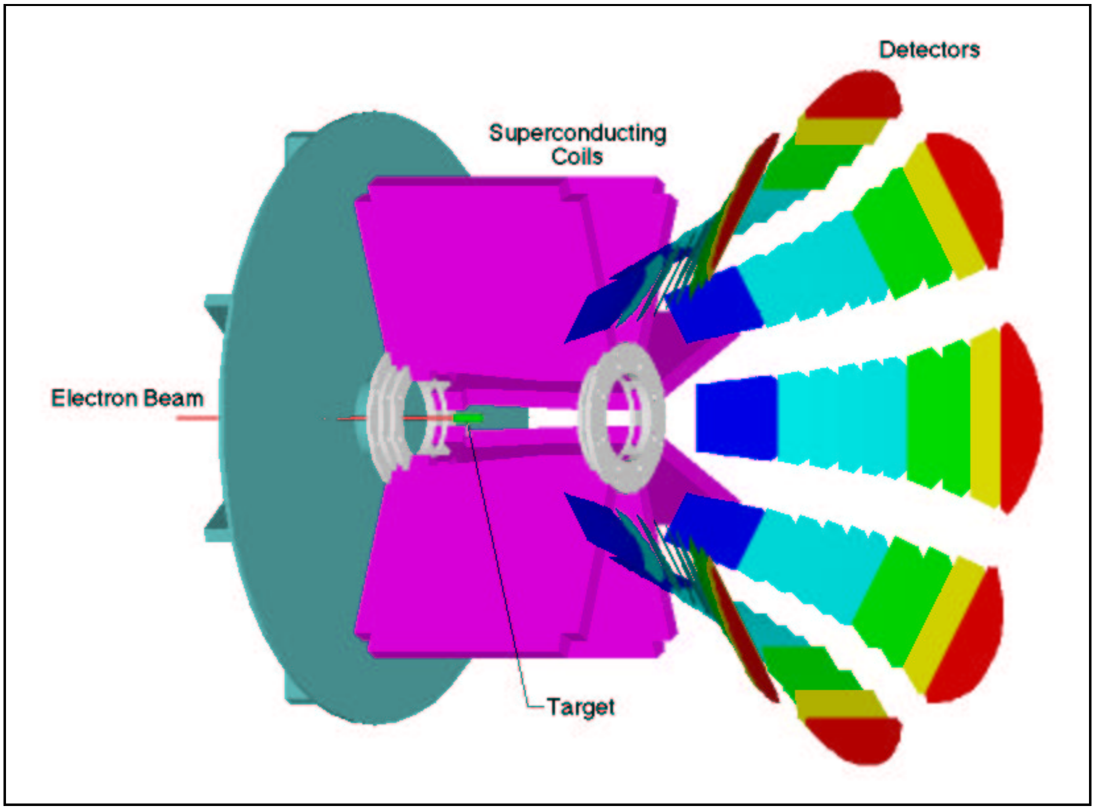

G^0 Apparatus (forward configuration)

- *Forward scattering on hydrogen* $[A_F(\varepsilon \sim 0.99)]$— Measure recoil protons from elastic scattering at $\theta_p \sim 70°$; corresponding to $\theta_e \sim 7°$.
  Q^2: 0.1 - 1.0 $(\mathrm{GeV}/c)^2$.

- *Backward scattering on hydrogen* $[A_B(\varepsilon \sim 0.2)]$— Measure scattered electrons at $\theta_e \sim 110°$ at three different beam energies.
  Q^2: 0.3, 0.5, and 0.8 $(\mathrm{GeV}/c)^2$.

- *Backward scattering on deuterium* $[A_d(\varepsilon \sim 0.2)]$— Identical measurement technique as in the backward hydrogen running.
  A_B and A_d depend differently on G_A^e.

Projected Errors on G_E^s, G_M^s, and G_A^e

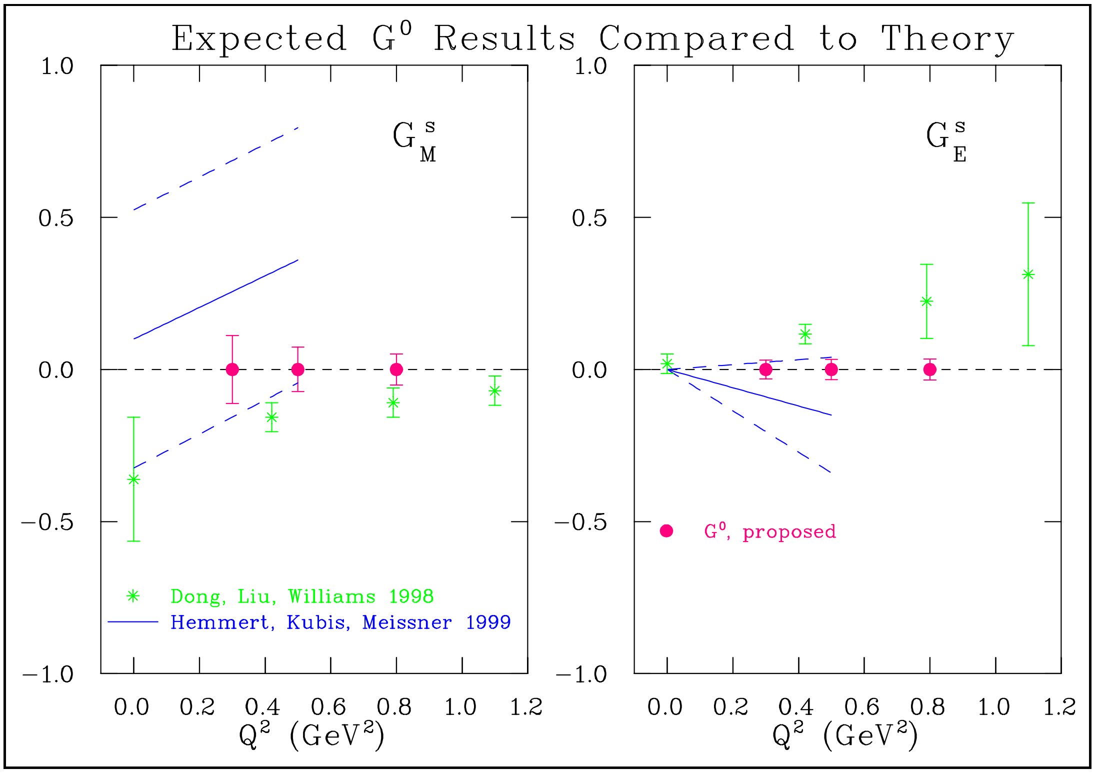

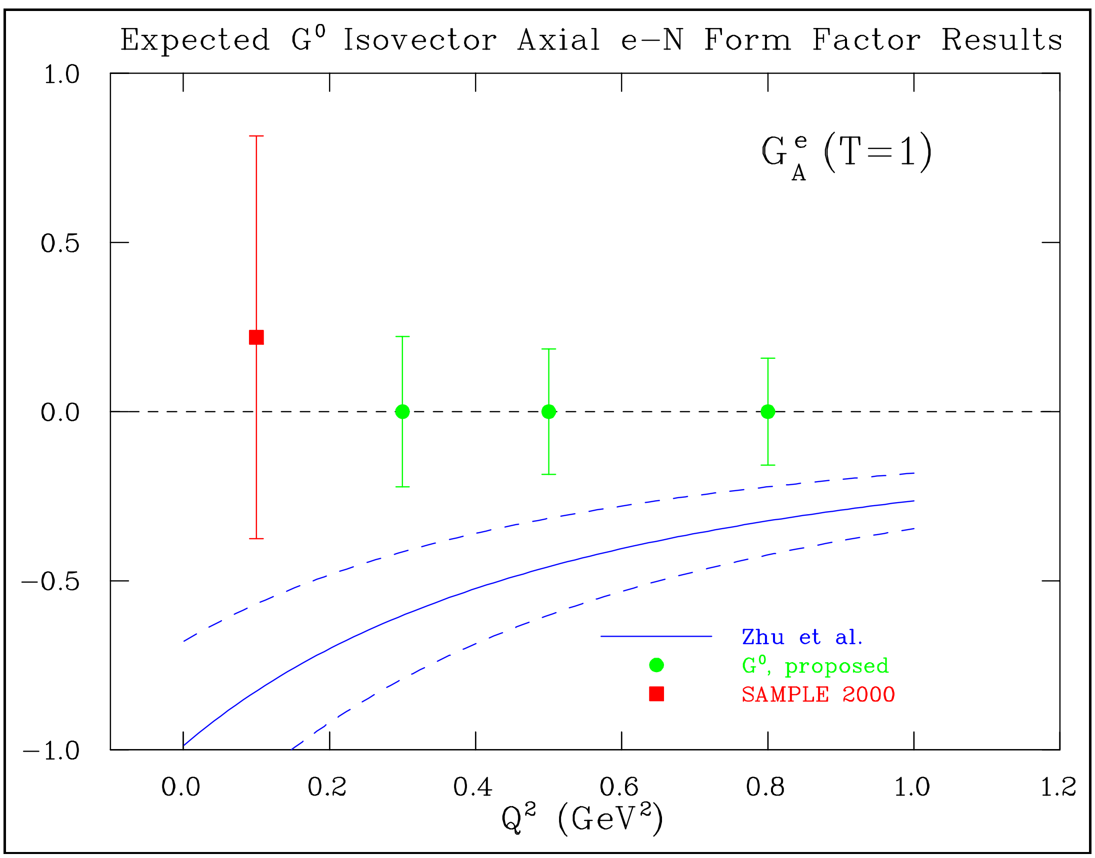

G^0 Apparatus

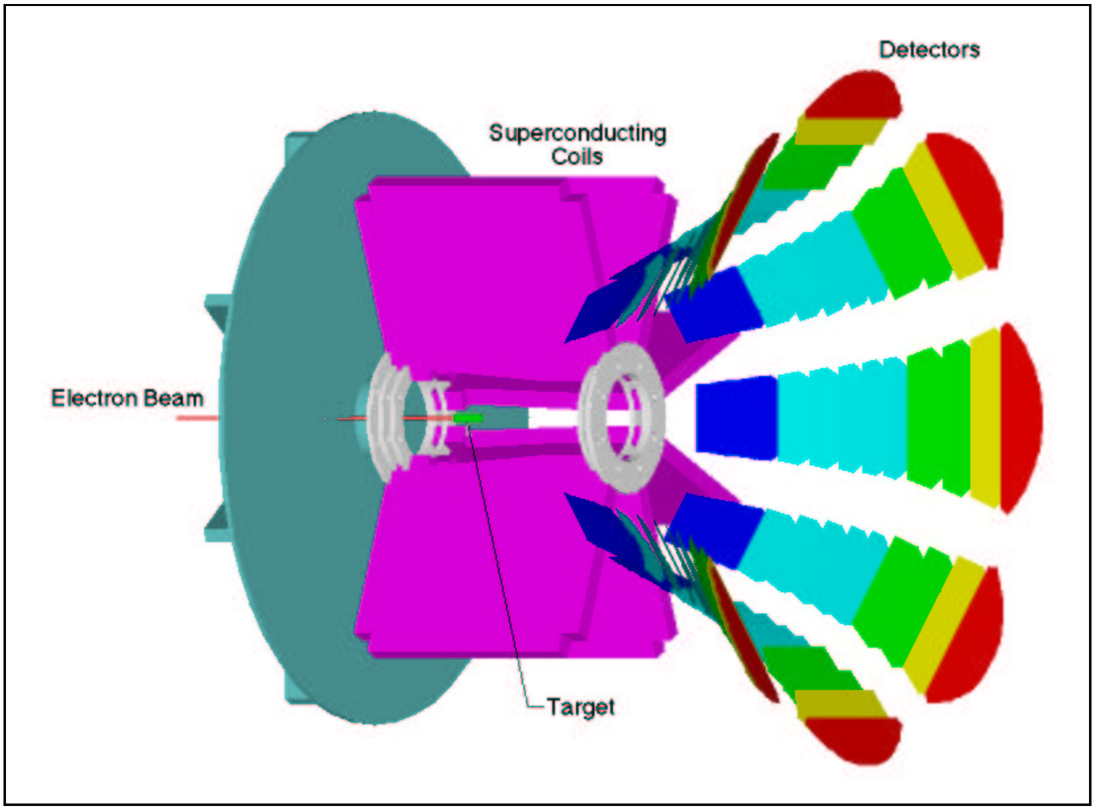

G^0 Apparatus (forward configuration)

- High intensity polarized electron beam with a unique time structure—40 μA average current at a pulse rate 16 times lower than standard JLab beam (31 MHz instead of 499 MHz)
- High power liquid hydrogen target
- Toroidal superconducting magnetic spectrometer with 8-fold azimuthal symmetry
- Segmented focal plane made of scintillation detectors—segmentation provides Q^2 binning in forward angle measurement
- Custom electronics to allow high rate (> 1 MHz) counting and particle ID using TOF

G^0 2002 Commissioning Run Working Groups

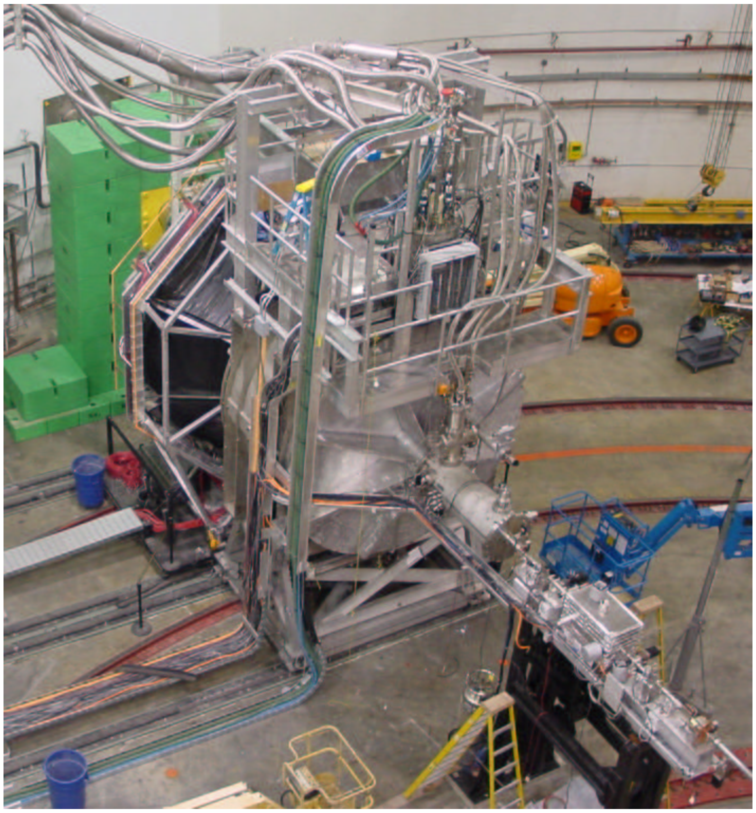

- Beam development

  Delivery of 40 μA parity-quality beam

- System Turn-on

  Detector calibration, SMS checkout, target commissioning, beam line commissioning

- Backgrounds

- Centering and Symmetry

- Systematics

- Asymmetry

- Empty Target

G^0 Beam Development

Delivery of 40 μA of G^0 time structure beam has been achieved.

The remaining development is directed at getting "parity quality".

1. Interaction of the 40 μA G^0 beam with beam for halls A and B
2. Helicity-correlated feedback systems
3. Adiabatic damping
4. Measurement and reduction of beam halo
5. Development of the beam pick-off signal (YO)
6. Betatron matching in the accelerator and BSY
7. Beam energy measurement

Helicity-Correlated Feedback Systems

- IA cell:

  The slope of IA cell voltage to the charge asymmetry has been unstable, but had periods of stability. It also shows a beam current dependence.

  Also, there are position variations caused by the IA cell (unsure of cause).

- G^0 PZT & Common PZT:

  One of the two actuators (the X actuator) on the G^0 PZT had been not working (replaced on 17 December).

  There are correlations between the X and Y modulation axes, as well as charge asymmetries induced by the position modulation.

  The G0 PZT has been shown to be stable on the order of three hours but is unstable day to day. Values can range from a couple 1000 ppm one day to negative 1000 ppm the next. The common PZT also is not consistent day to day but we do not have much data from it.

We have been able to operate the charge feedback for some of the overnight asymmetry runs.

G^0 SMS Status

- Limited to 4500 A (90% design current) during October-December
- Commissioned for running at 5000 A at the end of December

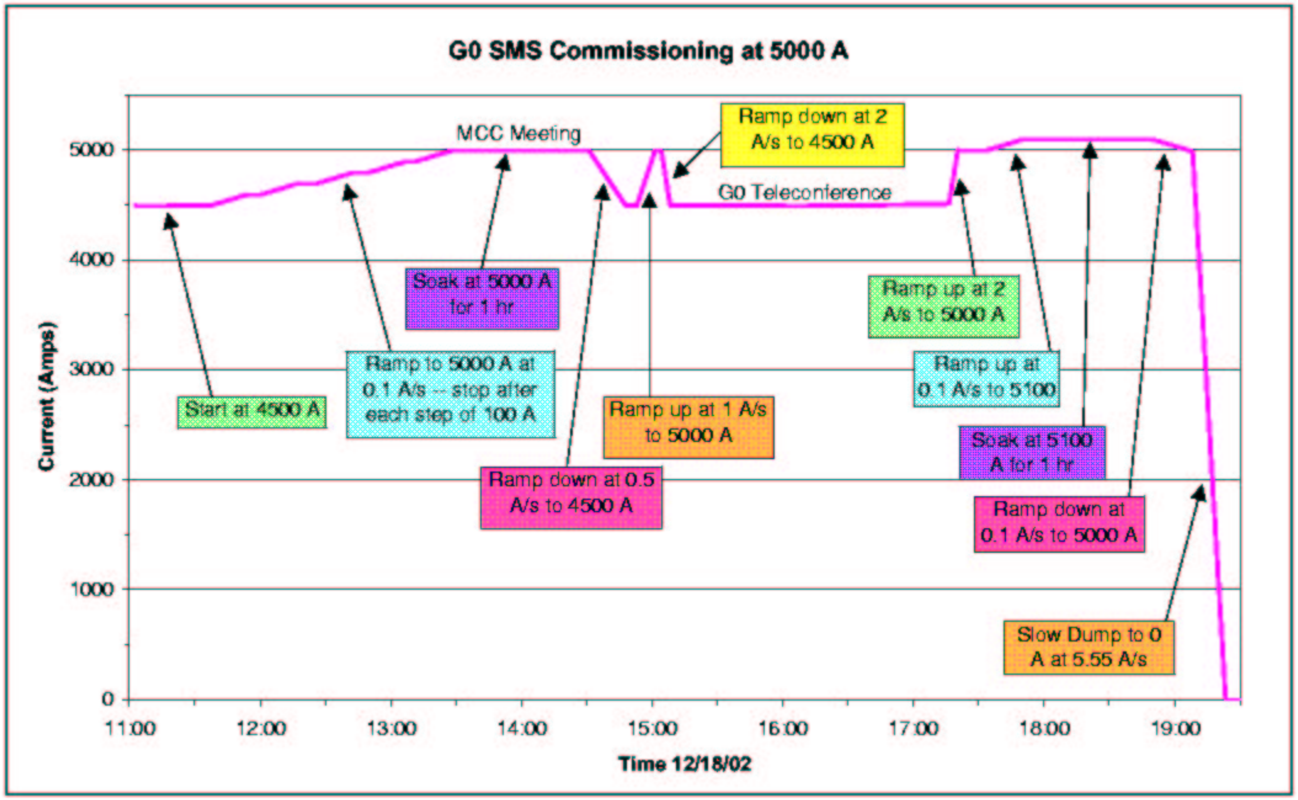

- Before the next commissioning run, the quench detection system will be modified (relocation of the "safety resistors" on the voltage taps outside of the cold mass).

G^0 Target Status

- The density fluctuations appear to be negligible at the operating parameters (40 μA beam, 30 Hz pump speed, 2×2 raster).

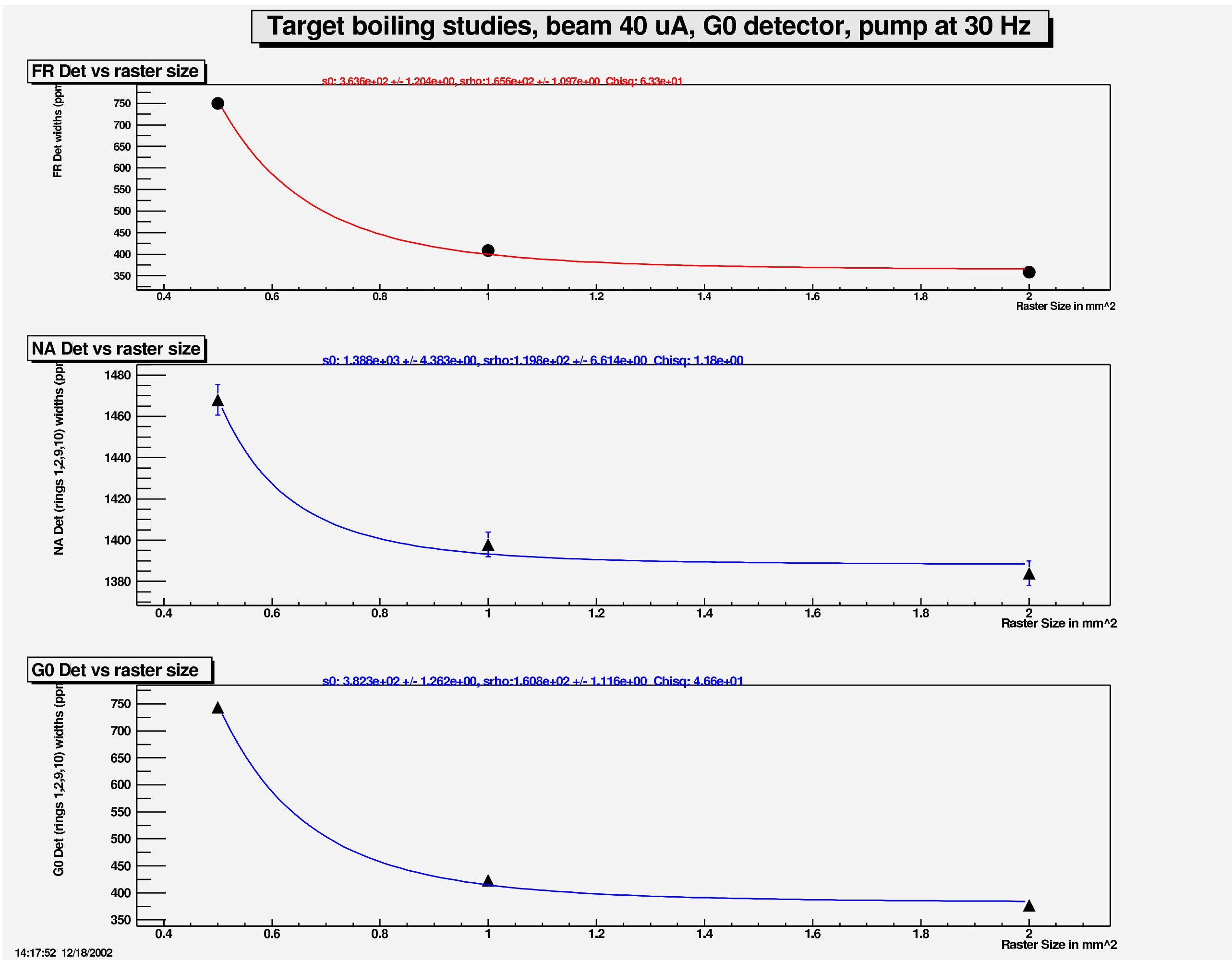

Detectors and Electronics

There are eight detector packages (Octants) each containing 32 scintillators arranged as sixteen front-back pairs. Each scintillator is instrumented with a PMT at either end.

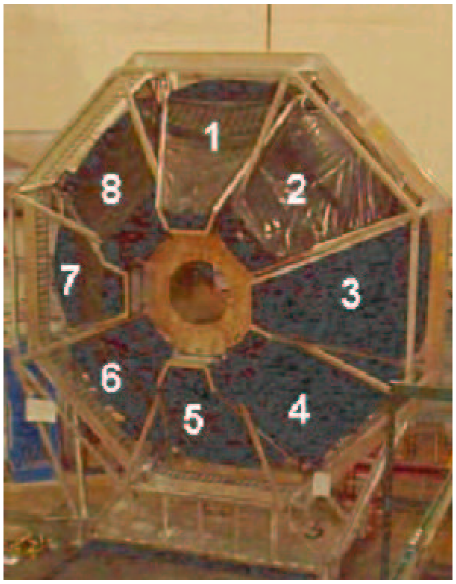

The signals from the four PMTs are used to determine the particle time of arrival at the focal plane with respect to the beam pulse; the TOF is then histogrammed and the electronics reset for the next beam pulse.

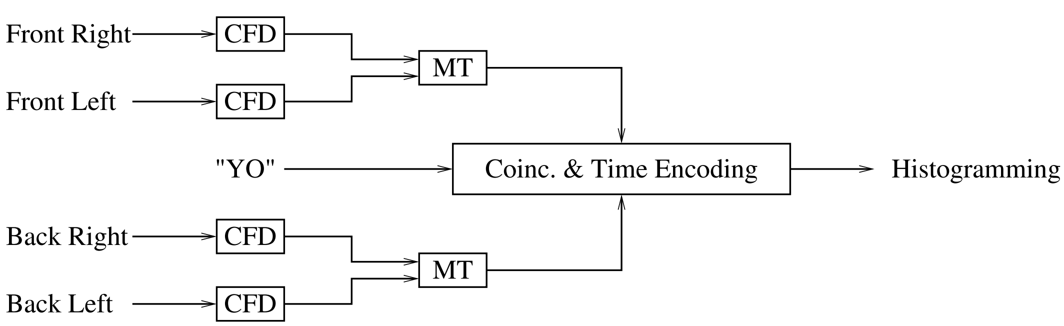

Time of Flight Spectra

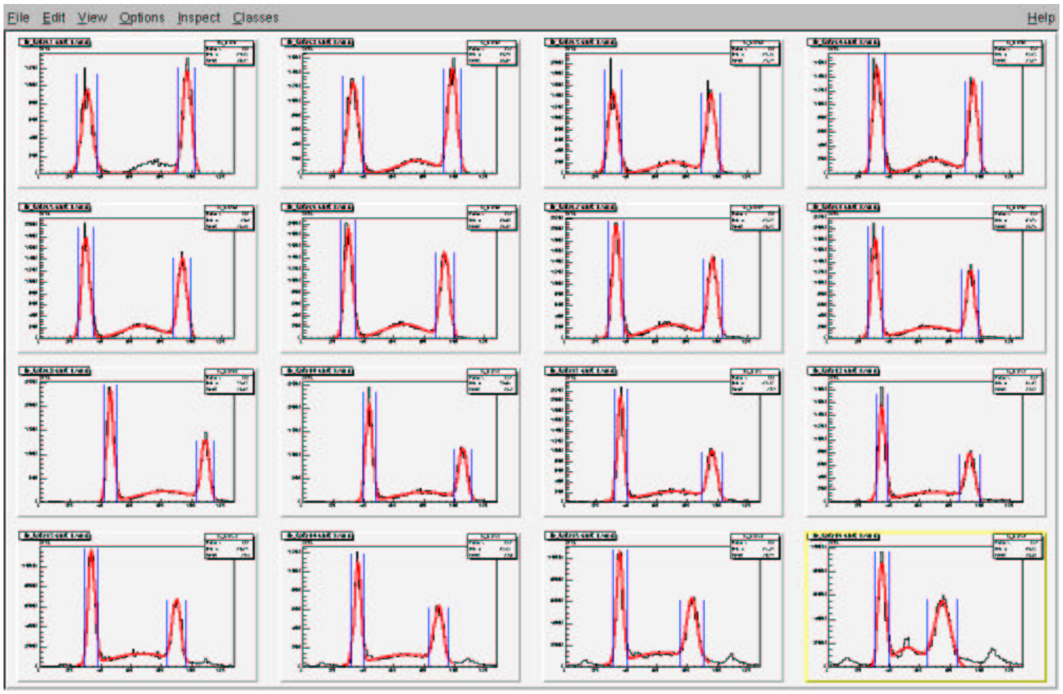

- The peaks shown are (left to right) the pions, the inelastic protons, and the elastic protons.
- The acceptance of the G^0 is such that the inelastic protons in a detector are at a higher Q^2 than the elastics and so arrive earlier.

Detector Status

- Need the signals to be high enough above the thresholds to minimize false asymmetries

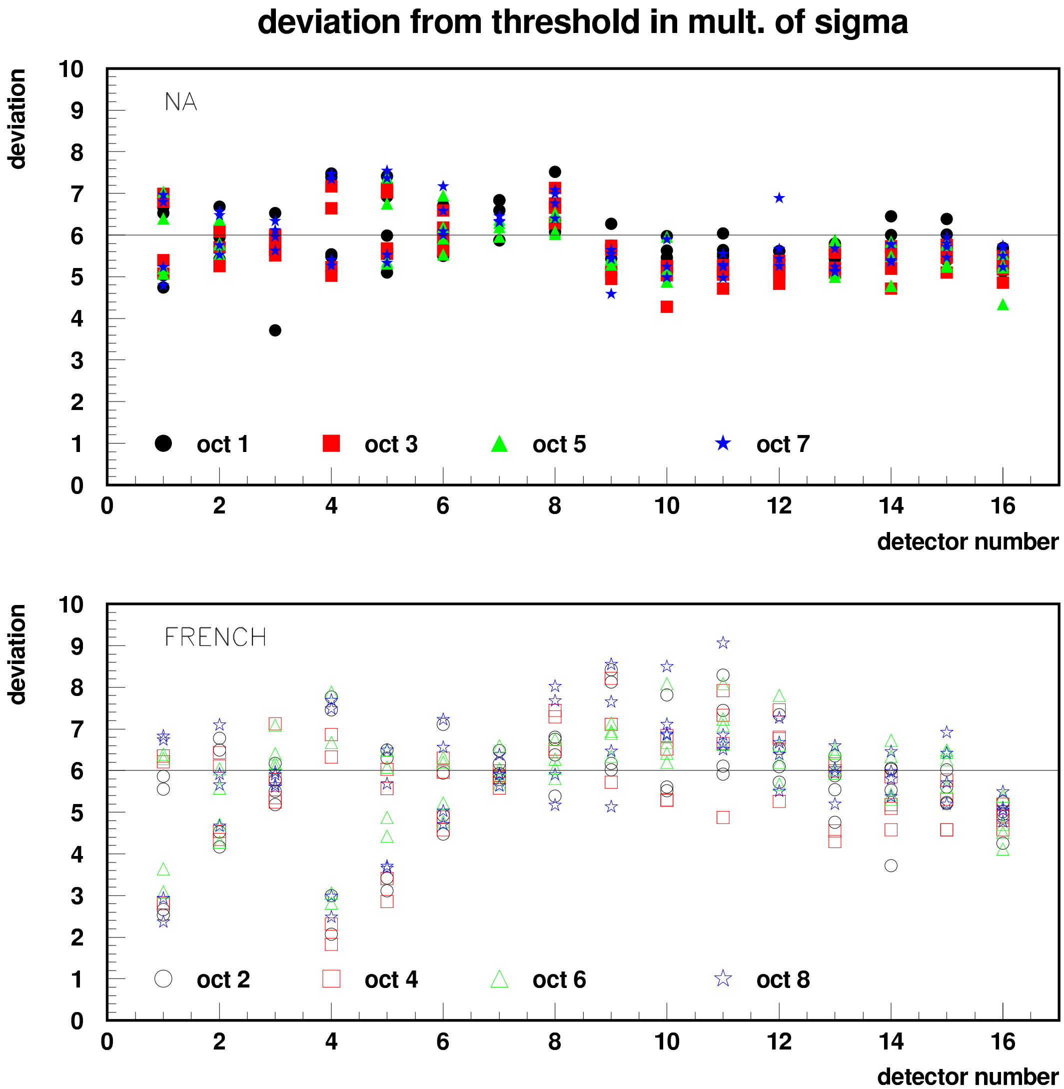

- The false asymmetry due to rate-dependent gain fluctuations (assuming a charge asymmetry of 500 ppm) for a signal amplitude of 6 σ is less than 10^{-13}
- G^0 can tolerate a signal height above threshold of 3 σ which leads to false asymmetries of the order 10^{-9}

But, the anode current must be kept small to not damage the PMTs.

Background Shielding Installation

- Based on measurements made in the first months of running, the projected anode currents of the largest detectors would have been too high ($\sim 400\ \mu$A) at 40 μA at the nominal gain settings.
- The nominal gain can be reduced by 2 (changes the signal height from 6σ above threshold to 3σ).
- The anode current is dominated by pulses below the discriminator threshold.
- Radiation simulations suggested that the largest contribution to this background was photons coming from the downstream beampipe.
- The downstream beamline has been surrounded by a four inch thick lead shielding box.
- The effectiveness of the new shielding is being evaluated.

Deadtime Studies

- Deadtime has been studied using the residual dependence of the detector asymmetry on the charge asymmetry at different beam currents

  Residual dependence at 15 μA beam current

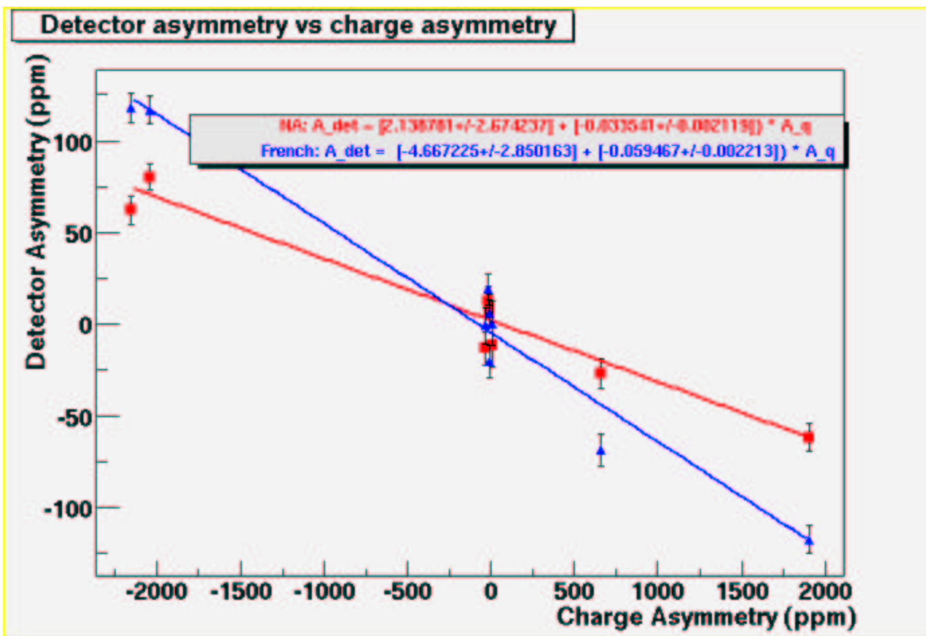

- The slope shows a linear dependence on beam current
- The slopes of the individual detectors show a similar distribution to that of the single CFD rates, which are not included in the first stage deadtime correction
- Analysis of this data is in progress

Q^2 Determination

By comparing measured versus simulated proton-pion TOF difference vs. magnetic field setting, the mean Q^2 per detector is determined. Preliminary analysis results show a precision on the Q^2 of about 2%.

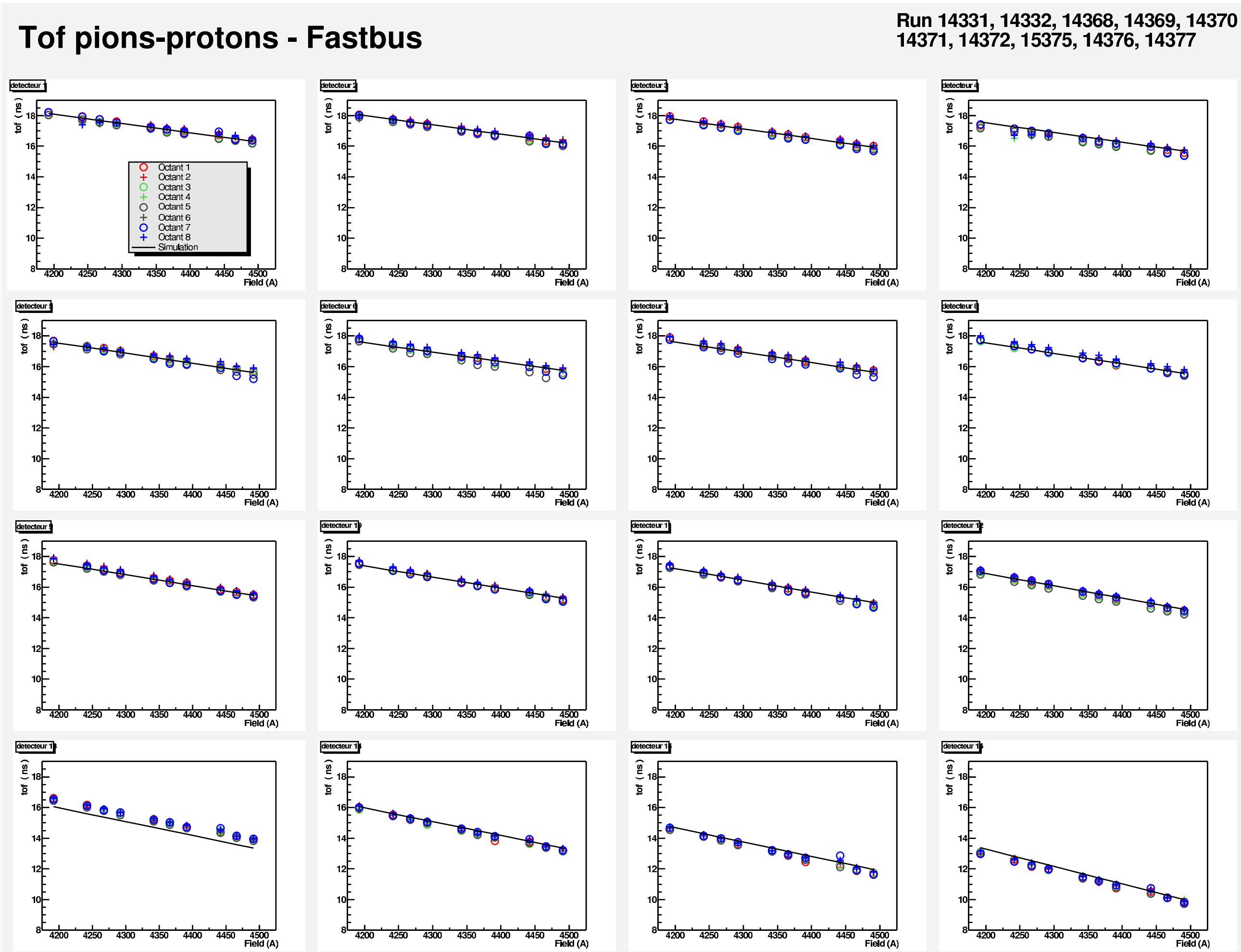

Symmetry and Centering

- There is a central region in which the detector responses are flat with respect to beam motion.

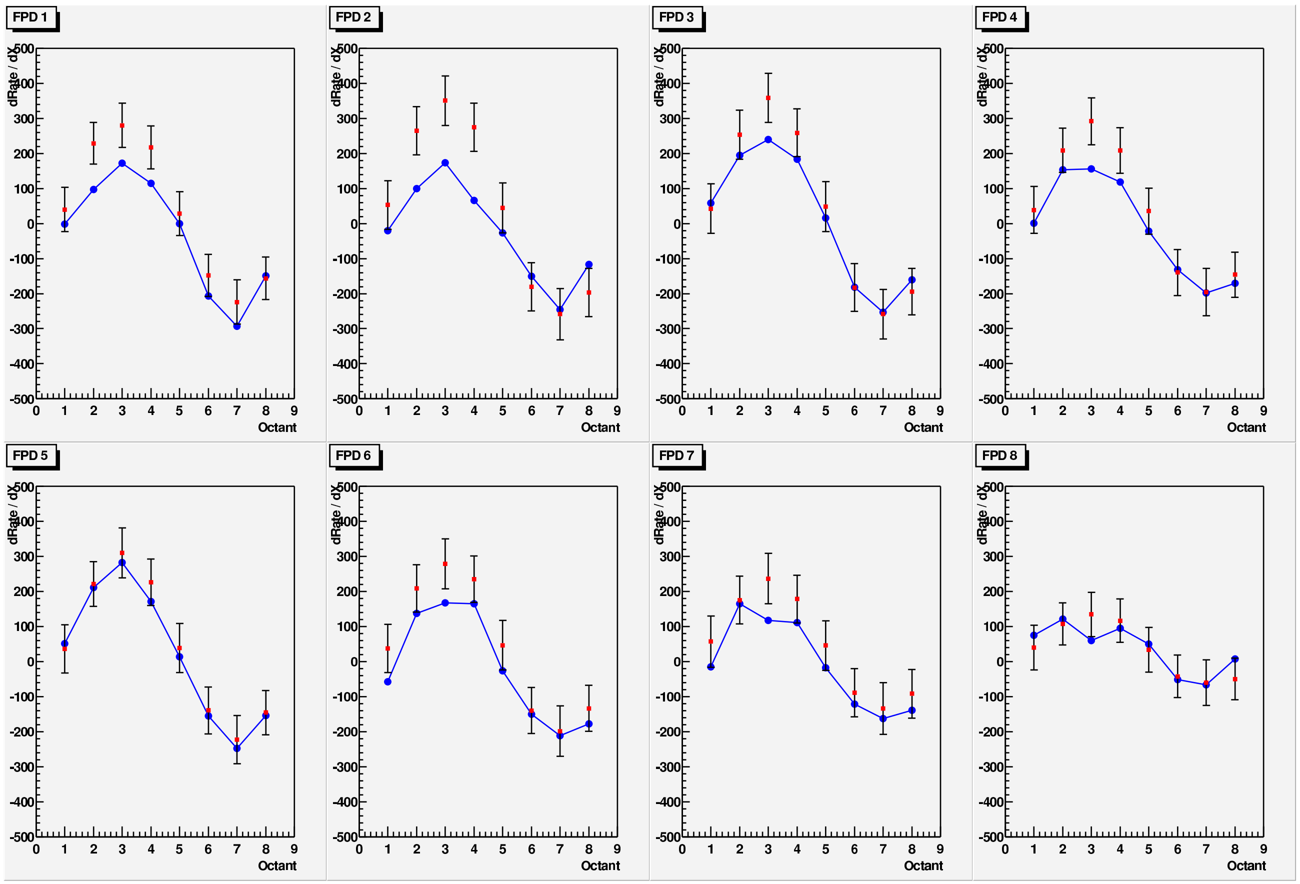

Changes in detector rates for changes in the X position of the beam versus octant number plotted for detectors 1 - 8. The blue lines are Monte Carlo simulation of the sensitivities.

Beam Polarimetry

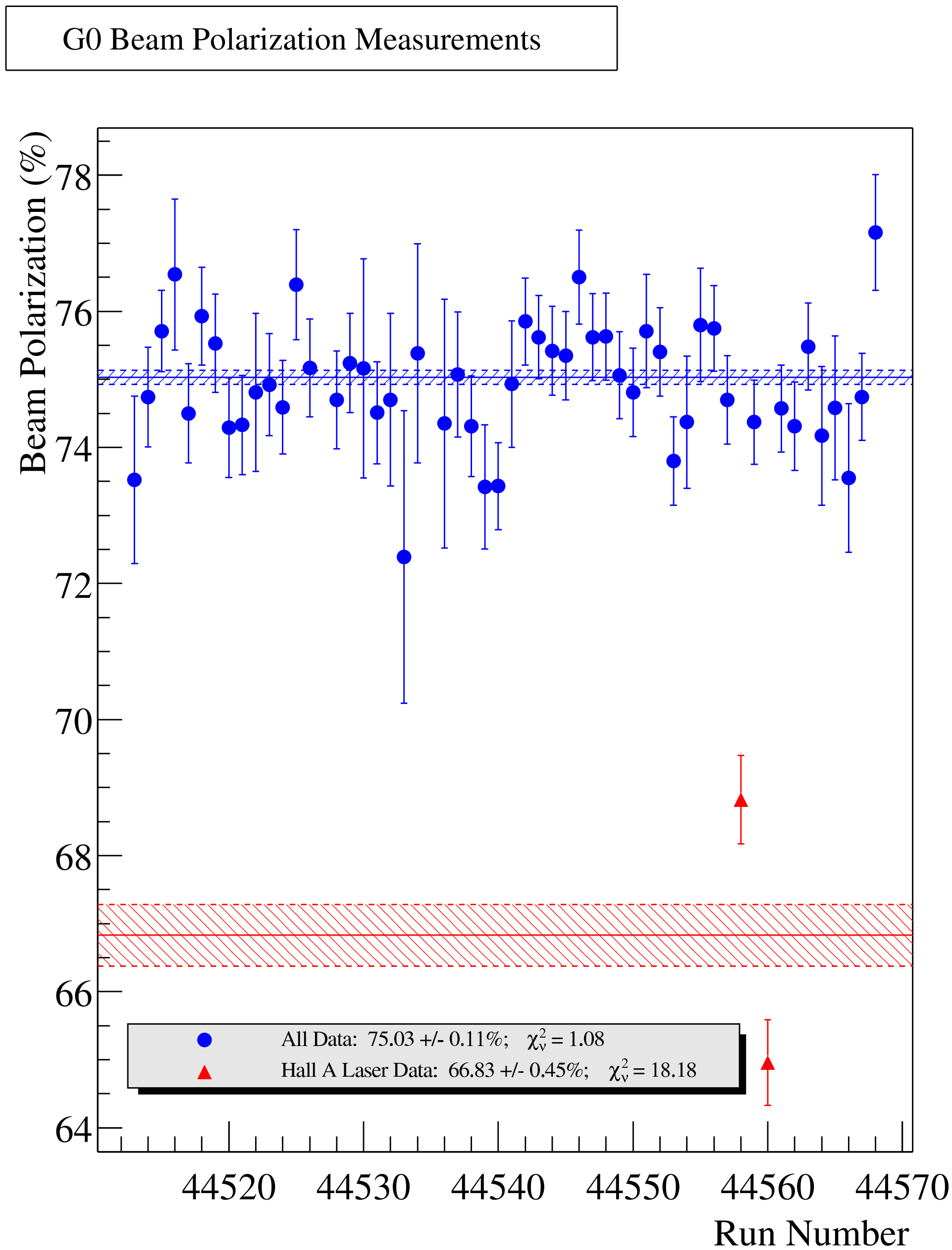

Detector Asymmetries

We have taken several long asymmetry runs with the insertable waveplate in and out.

For the SMS current at 4500 A and beam currents of about 13-15 μA, the detector asymmetries (averaged over 10 hour-long runs) are shown compared to simulation of statistics from 40 μA beam, $I_{SMS} = 4500$ A and 5 full days statistics.

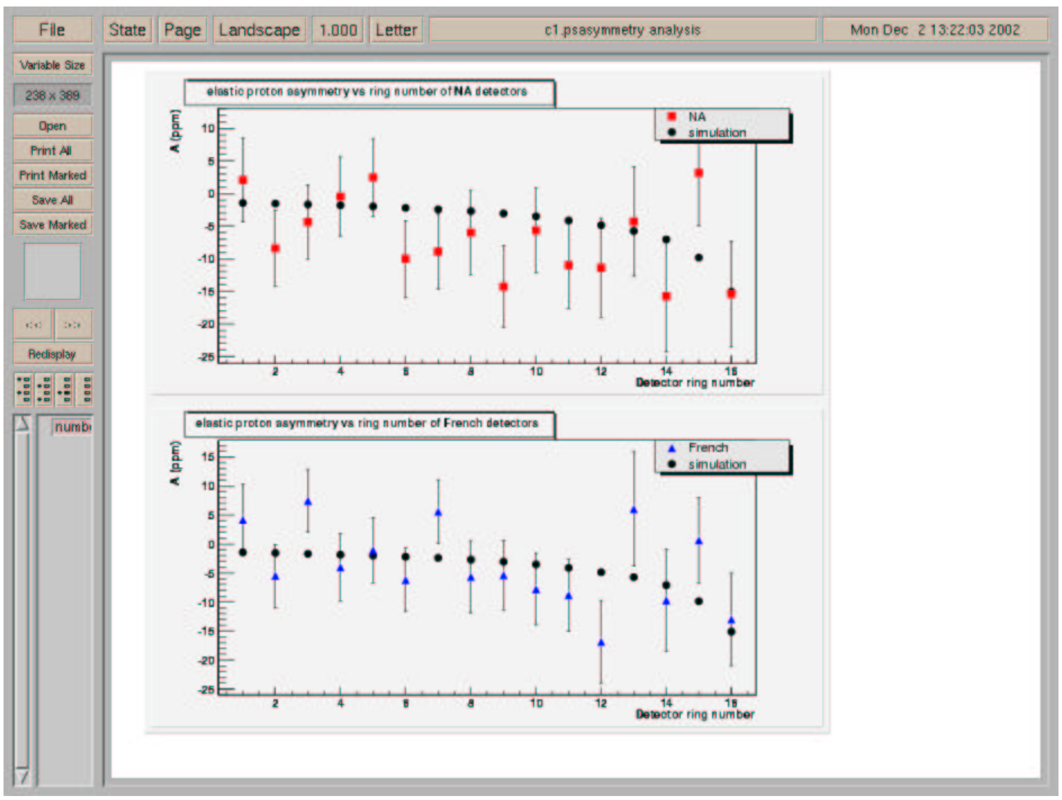

Empty Target

- The hydrogen cryotarget is allowed to boil off, then the target loop is operated as a cooled hydrogen gas target.

  By using two different temperatures for the hydrogen gas, different target densities are possible to aid in extracting the contribution from the target windows.

- Data with a hydrogen loop temperature of 26 K and pressure 18.5 psig was taken. The density of the gas is 3.34% that of the LH2 target density.

- A higher temperature target (35 K) was made but no data was collected due to beam problems. Density of this target is about 2.4% of the LH2 in running conditions.

- Expect to return to these measurements near the end of January.

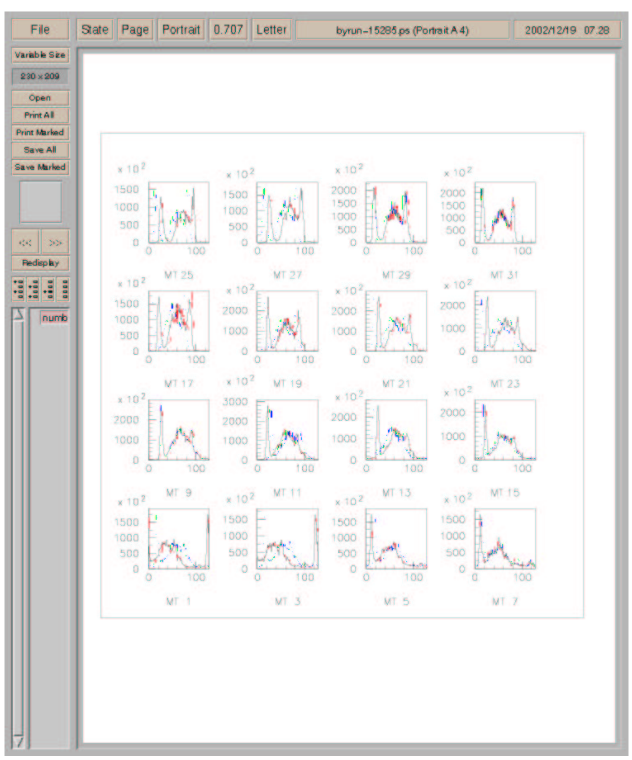

Plans for the remainder of the run

- Recalibration of Detector at $I_{SMS} = 5000$ A
- Evaluation of the new beamline shielding
- Continued development of 40 μA "parity quality" beam.
- Improved understanding of helicity control devices
- "Adiabatic damping" studies
- Q^2 determination at 5000 A in SMS
- Asymmetry data collection
- Studies of the deadtime
- Beam Energy Measurement
- Empty target running: H2 gas at two temperatures